ANALYSIS OF STRONG MOTION RECORDS FROM PARKING STRUCTURE DURING THE JANUARY 17TH NORTHRIDGE EARTHQUAKE

S. Hilmy, S. Werner, A. Nisar and J. Masek
Dames & Moore

ABSTRACT

The parking structure studied in this investigation is the first parking structure from which significant strong-motion data has been obtained during January 17, 1994 Northridge earthquake. Although the structure did not suffer significant damage, the study of the recorded motions was conducted to evaluate the seismic response of parking structures during strong ground shaking and the adequacy of the current seismic design provisions for such structures.

An important element of this research project was the use of system identification of the recorded motions in the parking structure, in order to estimate normal modes of vibration excited in the structure during the Northridge Earthquake. These normal modes were then used to calibrate a detailed finite element model of the structure which, in turn, was used to carry out detailed seismic analyses of the structure. The analyses indicated that proper modeling of all the elements of the parking structure including soil flexibility led to reasonable prediction of the main dynamic response characteristics of the parking structure. From this, several design recommendations were proposed in this study to improve the current modeling techniques and the code design provisions of parking structures.

INTRODUCTION

The extensive damage to parking structures during the Northridge earthquake, resulted from several unique characteristics of such structures (Ref. 1). For example, many of the damaged parking structures were constructed from precast concrete components which lacked adequate strength, ductility and redundancy. In addition, the architectural configuration of the sloped ramps in parking structures and the existence of the deep spandrels attached to the perimeter columns results in short effective lengths of the columns. The shear demands for these short columns increase significantly as their length decreases. The concrete ramps in parking structures form a connecting link between floors that is not typically modeled in the seismic design and analysis process. Sloped ramps with a large span-width ratio may experience large floor accelerations and may result in more flexible response and high seismic stresses in certain members. Another unique feature of the parking structure is the existence of long spans and open architecture, both to reduce construction cost and to increase parking space. Parking structures typically lack interior nonstructural elements and are subjected to effectively larger forces and deformations. Finally, separation joints in older parking structures were often insufficient to prevent pounding, which was observed in many instances.

The poor performance of many parking structures during the January 17th, 1994 Northridge Earthquake demonstrates the need for further evaluation of the current seismic analyses and design procedures for such structures. An important vehicle for improving these procedures and for understanding the seismic response characteristics of parking structures is the compilation and analysis of strong motion records from such structures using sound analysis procedures. Unfortunately, there had been no known evaluation of recorded motions in parking structures during the past earthquakes. In fact, the structure investigated in this project is the first parking structure in which earthquake motions had been recorded.

A set of 14 strong motion records was obtained by the Strong Motion Instrumentation Program (SMIP), of the California Department of Mines and Geology, at a 6-story parking structure in Los Angeles during the Northridge earthquake. The recorded horizontal acceleration time histories had peak values of 0.29 g at the base of the structure and 0.84 g near the center of the roof diaphragm. One of the sensors, which was attached to the top of the roof parapet indicated acceleration as high as 1.21 g. However, the structure did not suffer from significant structural damage during the earthquake. The main objective of the study summarized herein was to study these recorded motions using the MODE-ID method and to investigate the adequacy and accuracy of the finite element modeling techniques currently used in the analysis of these structures. Based of the assessment of the behavior of the parking structure and study of the recorded motion, demand/capacity ratios of the structural members have been compared to allowable code values.

DESCRIPTION OF THE PARKING STRUCTURE UNDER INVESTIGATION

The overall structural configuration and the location of accelerometers are shown in Fig. 1. The parking structure is located near downtown Los Angeles. It is a six story reinforced concrete structure that is rectangular in plan, and has plan dimensions of approximately 307 feet in the east-west direction and 260 feet in the north-south direction. The structure has seven levels of parking with a total usable area of approximately 550,000 square feet. The typical floor height of the structure is 10 feet. The building was constructed in two phases. The first three stories were constructed in 1977 "Phase I" construction project. These stories contain a 5-inch cast-in-place post-tensioned concrete slab spans between adjacent precast concrete beams, which are spaced at 18 ft. o.c. The lateral load resisting system consists of cast-in-place shear walls. Each wall is 32.5 feet wide, and 14" thick. There are two interior walls (72' long and 16" thick) along the east-west direction. The soil at the site consists of alluvium soil on a deep layer of firm sand. All columns are supported on drilled bell caissons.

In 1979, a "Phase II" project resulted in construction of three additional levels above the original parking structure, with a similar architectural layout to the existing structure. However, during this phase, cast-in-place concrete was used for all additional columns and walls. The interface between Phase I and II construction is provided by roughening the existing concrete surface and by providing full strength butt welding of existing and new reinforcements. The exterior spandrels at the south and north sides are separated from the columns. However, the spandrels at the east and west sides are connected to the shear walls with continuous steel dowels to provide flexural continuity at the beam-wall joints.

Photo #1 shows a view of the structure. One important characteristics of the parking structure is that the interior prestressed beams are seated on neoprene bearing pads at the columns corbels, with no positive ties between the beams and columns. The slabs are connected to the columns with $^3/_4$ inch diameter coil inserts that are embedded 6 inches into the columns and are connected to $^3/_4$ inch diameter threaded rods that are embedded three feet into the slab; the typical connection between the precast concrete columns and cast-in-place walls is provided through steel dowels and shear keys.

Photo 1. View looking northeast

STRONG MOTION DATA

The parking structure is located approximately 31 km from the epicenter of the Northridge earthquake which occurred at 4:30 a.m. on the morning of January 17, 1994, and had a moment magnitude (MW) of 6.7. The California Division of Mines and Geology deployed a total of 14 strong motion accelerometers within the structure whose locations along the first floor, fourth floor, and roof are shown in Fig. 1. This instrumentation system has been designed to measure (a) horizontal translations (in two orthogonal directions) and torsional rotations of each instrumented floor, (b) vertical translations of the first floor, together with rocking rotations of the floor about the north-south axis; © in-plane diaphragm deformations in the north-south direction, and (d) out-of-plane bending deformations of the parapet on the north side of the roof. In addition, a single vertical accelerometer is located on the roof.

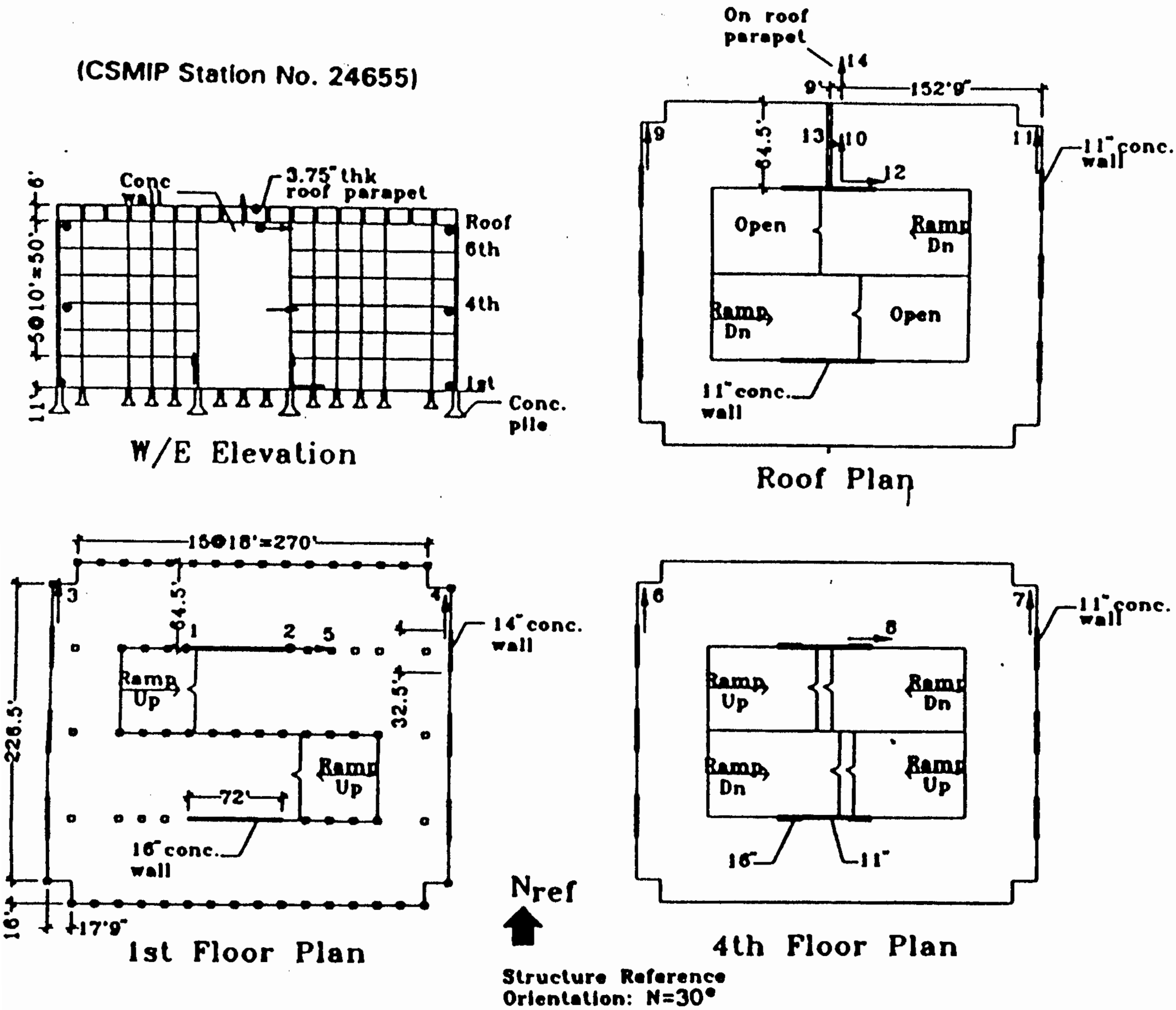

Figure 1. Structural Configuration and the Location of Accelerometers

The motions recorded at the base of structure were moderately strong, with peak horizontal accelerations of 0.29 g and 0.15 g in the north-south and east-west directions respectively and peak accelerations of the two vertical accelerograms of 0.22 g and 0.11 g. These motions were amplified substantially over the height of the structure, attaining peak horizontal roof accelerations of 0.55 g and 0.31 g in the north south and east-west directions. The north-south accelerations at the mid-length of the roof was amplified still further with a peak acceleration of 0.84 g. In addition very strong horizontal motions were recorded on the north parapet (with peak acceleration of 1.21 g), and strong vertical motions of a roof girder were also recorded (peak acceleration = 0.52 g). The duration of the strong shaking segment of the recorded motions was in the order of 12-13 sec. A comparison between the time-history acceleration records at different stations is shown in Fig. 2. The generated response spectra curves of the recorded motion at the base of the structures, along the north-south and east-west directions, are shown in Fig. 3.

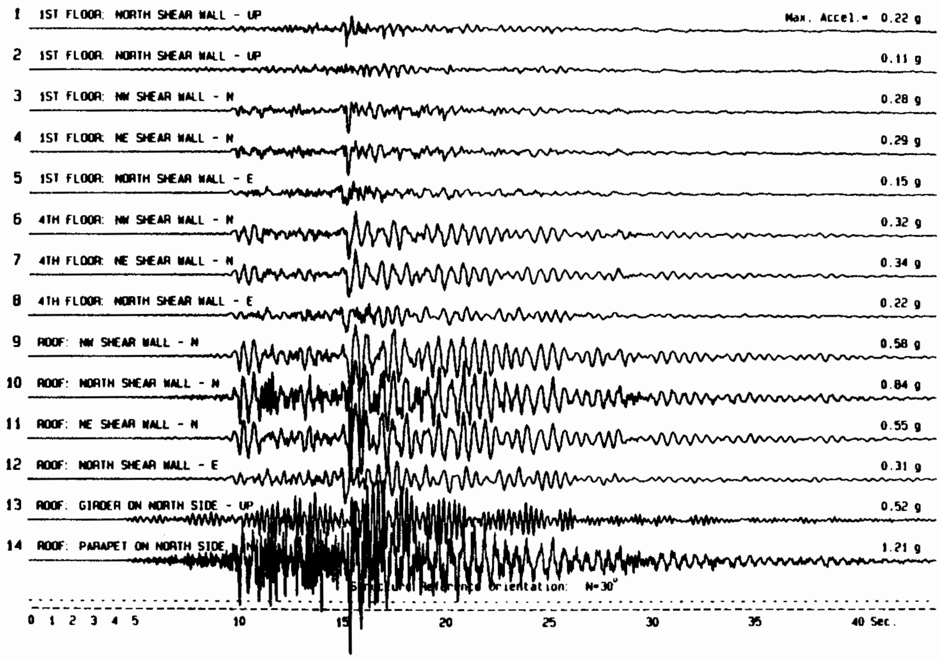

Figure 2. A Comparison Between the Time-History Acceleration Records at Different Stations

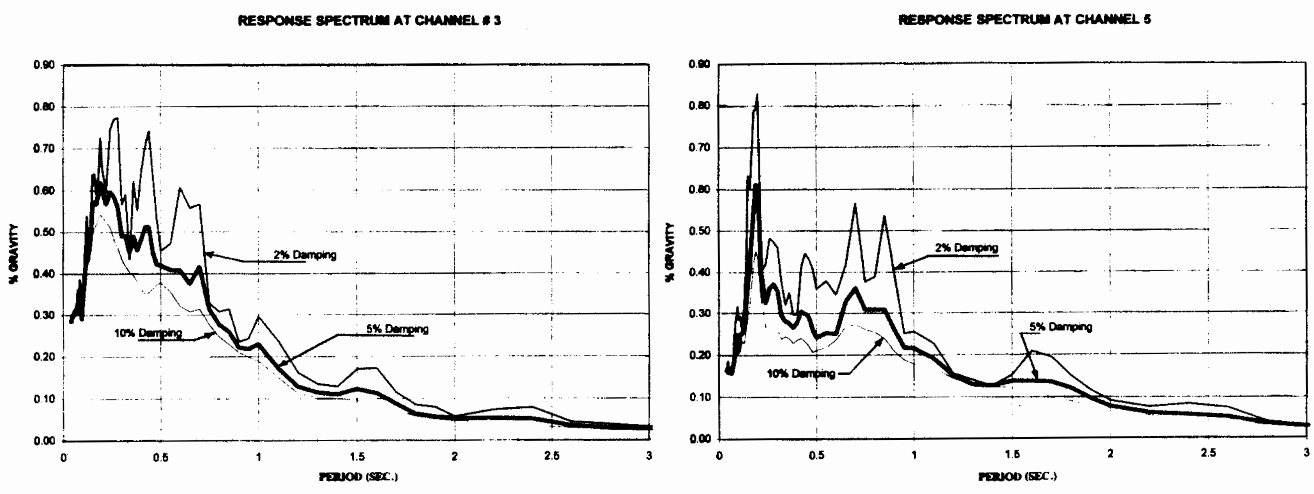

Figure 3. Generated Response Spectra Curves of Recorded Motions

SYSTEM IDENTIFICATION OF RECORDED MOTIONS

In order to estimate the modal parameters for the modes of vibration of the structure during the Northridge earthquake the MODE-ID system identification procedure was applied to the strong motion records. This procedure involved three main steps: (1) seismic response analysis was carried out by examining the accelerogram records and by computing transfer functions. These transfer functions were computed as ratios of the Fourier Amplitude Spectra (FAS) of the recorded motions at the upper floors to the FAS of the motions of the ground floor; (2) model parameters that were identified by MODE-ID were the natural period, mode shape, damping ratio, and participation factors for each significant mode of vibration; and (3) assessment of the adequacy of the identified model, by comparing the computed model motions to the recorded motions; assessment of the relative contributions of the structure's pseudostatic response and its response in each mode of vibration to its total response; and interpretation of the relative translational, torsional, and rocking contributions to the response of the parking structure in each mode.

The structural response to the input motions is assumed to consist of two components; the pseudo-static component and the dynamic component. The pseudostatic component represents the "quasi-static" contributions of the individual support motions to the building's total response (neglecting inertial and damping effects). It can be visualized as a time-dependent "reference" position of the structure whose deformed shape at each instant of time depends on the instantaneous position of the structure's supports. This pseudostatic response is represented as the product of a pseudostatic matrix and the vector of input motions. The dynamic response component represents the contributions of the structure's modal vibrations about its pseudostatic reference position. The model parameters that are used to compute the dynamic component are the natural period, damping ratio, input participation factors, and mode shape amplitude for each significant mode excited by the earthquake. The pseudostatic and normal mode parameters are estimated by a least-squares output-error method, in which MODE-ID uses an optimization algorithm to compute the "best" matching of the measured response (Ref. 2). Within a Bayesian probability framework, the estimated parameters can be viewed as most probable values based on the given data (Ref. 2).

For the parking structure under investigation, it was not necessary to identify the pseudostatic matrix using MODE-ID; rather, the matrix was calculated directly based on the assumption that the base of the structure was rigid. The pseudostatic matrix and then one mode at a time were successively incorporated into the model, and the modal parameters identified from each MODE-ID run were used as input to the next run with one additional mode included. This process led to the identification of the modal parameters for each significant mode, such that the resulting building model (which also includes the pseudostatic matrix) minimized a measure-of-fit parameter $J(\theta)$. This parameter is defined as the ratio of the sum of the output errors to the sum of the squares of the measured accelerations, i.e.,

$$J(\theta) = \frac{1}{V} \sum_{i=1}^{NR} \sum_{n=0}^{NT} [a_i(n\Delta t) - \ddot{y}_i(n\Delta t, \theta)]^2 \tag{1}$$

where

$$V = \sum_{i=1}^{NR} \sum_{n=0}^{NT} [a_i^2(n\Delta t)] \tag{2}$$

and

a_i, $\ddot{y}_i$	=	Measured acceleration and computed model acceleration for the ith output degree of freedom (where I= 1,2,- - - - - NR, which is the total number of output channels).
θ	=	Pseudostatic matrix elements and identified modal parameters.
Δt	=	Time step at which the recorded motions in the structure have been digitized (= 0.01 sec.).
n	=	Time step number ranging from 0 to NT, which corresponds to a total duration of NT x Δt sec.
V	=	Sum of the squares of the recorded accelerations.

Time-Invariant and Time-Varying Models

Both time-invariant and time-varying models of the parking structure were used to show how the modal parameters vary over time (as the intensity of the ground shaking varies), and to assess the degree to which nonlinear behavior may have played a roll in the structure's seismic response. Four time segments over which the strength of the shaking appeared to be clearly different were considered: (a) 10-15 sec., which corresponds to the initial buildup of the strength of the shaking; (b) 15-30 sec. which corresponds to the duration of the strongest shaking of the structure during the earthquake; © 30-40 sec., during which the shaking of the structure decayed to very low levels; and (d) 40-60 sec., when the structure was undergoing essentially free vibration under very low intensities of shaking. In addition to the time-invariant models, time-varying models were identified using overlapping sliding time windows with a duration of 5 sec. and an overlap of 2.5 sec.; i.e.10-15 sec., 12.5-17.5 sec., 15-20 sec., 17.5-22.5 sec., etc.

For both the time-invariant and time-varying models, the input motions to MODE-ID consisted of the horizontal motions recorded at the base of the structure, as well as the average (i.e., translational component only) of the vertical base motions. The output motions were considered to be the horizontal motions measured at all of the instrument locations above the base of the structure, as well as both sets of vertical motion records measured at the base.

The significant modes of vibration estimated for the parking structure include the effects of horizontal translation in the north-south and east-west directions, torsional rotation (about a vertical axis), and rocking of the structure about its north-south axis. The effects of rocking on the structural response in the east-west directions were estimated by computing an equivalent rigid body translational component of the mode shape amplitude at each instrumented floor due to rocking, i.e.

$$\phi_{R,i,n} = (\phi_{v2,n} - \phi_{v5,n}) \times H_i/D_{2-5} \qquad (3)$$

where, for the nth mode, $\phi_{R,i,n}$ is the mode-shape's east-west component of translation at the ith floor due to rocking of the base, $\phi_{v2,n}$ and $\phi_{v5,n}$ are the mode shape's vertical component of translation at the locations of Channels 2 and 5 along the base of the structure, D_{2-5} is the distance between Channels 2 and 5, and H_I is the height of the ith floor above the base.

Model Assessments

An important element of the MODE-ID process is an evaluation of how well the various models of the parking structure that were identified from each set of recorded earthquake motions represent the structure's seismic response during the Northridge Earthquake. This assessment was based on (a) the use of past experience (Ref. 4, 5) to evaluate whether the minimum value of $J(\theta)$ obtained for each model was sufficiently small to represent a good overall fit between the measured response of the structure and the computed model response; and (b) visual comparison of recorded and computed model acceleration time histories and their Fourier amplitude spectra, at selected locations in the structure. As part of this model assessment, we also evaluated the relative contribution of the pseudostatic response and each identified mode of vibration to the structure's seismic response. To accomplish this, we examined how much $J(\theta)$ decreased as the pseudostatic matrix and each identified mode were successively incorporated into the model.

Once a theoretical pseudostatic matrix for parking structure was developed, this matrix was incorporated into all time-invariant and time-varying models that were identified for the structure. For each time segment, a total of six modes of vibration were identified (Fig. 4). The first identified mode corresponds to the first translational mode of vibration in the north-south direction. At each instrumented floor, the north-south translational components of the mode shape amplitudes along the east and west faces of the parking structure are comparable to each other, increase nearly linearly with increasing height above the ground floor, and are much larger that the east-west translational components (which are essentially negligible). In-plane deformations of the roof diaphragm are relatively large for the 10-15 sec. time segment, and are somewhat smaller for the other time segments.

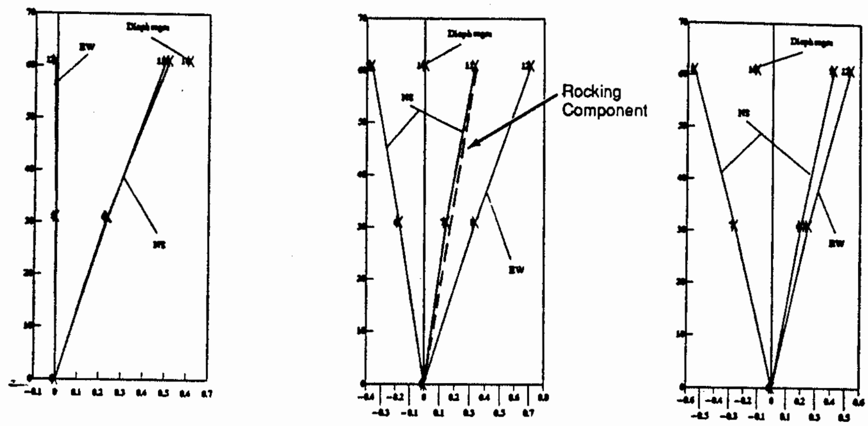

a) Mode 1: First North-South
(T=0.53 sec, ξ = 4.8 %)

b) Mode 2: First East-West
(T=0.42 sec, ξ = 4.6 %)

c) Mode 3: Torsional
(T=0.38 sec, ξ = 4.2 %)

Output \ Input	3	4	5	∇
6	1	0	0	0
9	1	0	0	0
7	0	1	0	0
11	0	1	0	0
10	0.5	0.5	0	0
8	0	0	1	0
12	0	0	1	0
1	0	0	0	1
2	0	0	0	1

Input Channels: 3, 4, 5, ∇

where ∇ = (Ch1 + Ch2)/2

Output Channels: 6, 9, 7, 11, 10, 8, 12, 1, 2

Pseudostatic Matrix

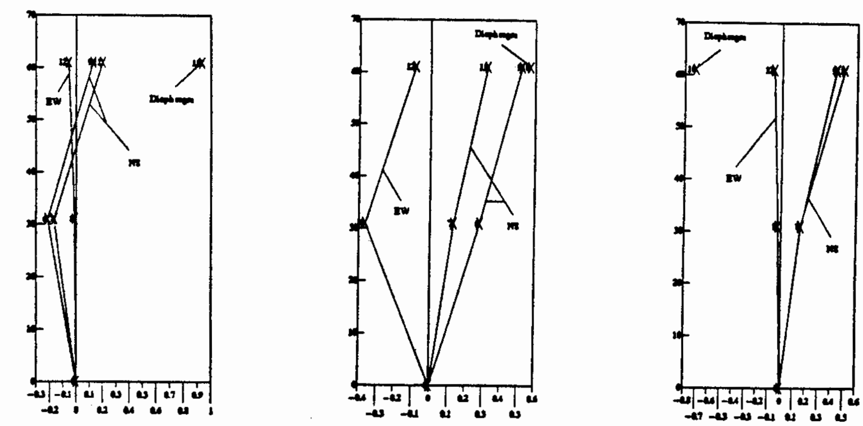

d) Mode 4: Second North-South
(T=0.18 sec, ξ = 5.0 %)

e) Mode 5: Higher Mode
(T=0.15 sec, ξ = 4.4 %)

f) Mode 6: Higher Mode
(T=0.12 sec, ξ = 1.7 %)

Figure 4. Identified Mode Shapes for Time Segment = 15-30 Sec., and the used Pseudostatic Matrix for the Rocking Base Model of the Parking Structure

Mode #2 is dominated by the east-west translational components of motion, which increase nearly linearly with increasing height above the ground floor, and contains some torsional rotations of the diaphragms, and only small translations in the north-south direction. The in-plane diaphragm deformation in this mode is small. Mode #3 features significant torsional rotations accompanied by only very small north-south translations. Mode #4 contains north-south translational components at the fourth floor that are of comparable magnitude but opposite sign to those at the roof. Modes #5, and #6 are higher modes.

Comparisons between Computed Model Motions and Recorded Motions

For each time segment, the time-invariant models comprised of the above six normal modes plus the pseudostatic matrix shown in Fig. 4 led to an excellent fit between the computed model motions and the recorded motions. This excellent fit is evidenced by: (a) the very low values of the measure-of-fit parameter, J(θ), which range from about 0.021-0.035 (where, from past experience, values of J(θ) of about 0.15 or less generally represent an excellent fit); and (b) very close visual comparisons of the time histories and Fourier amplitude spectra of the computed model motions and the recorded motions, as typified by the comparisons shown in Fig. 5.

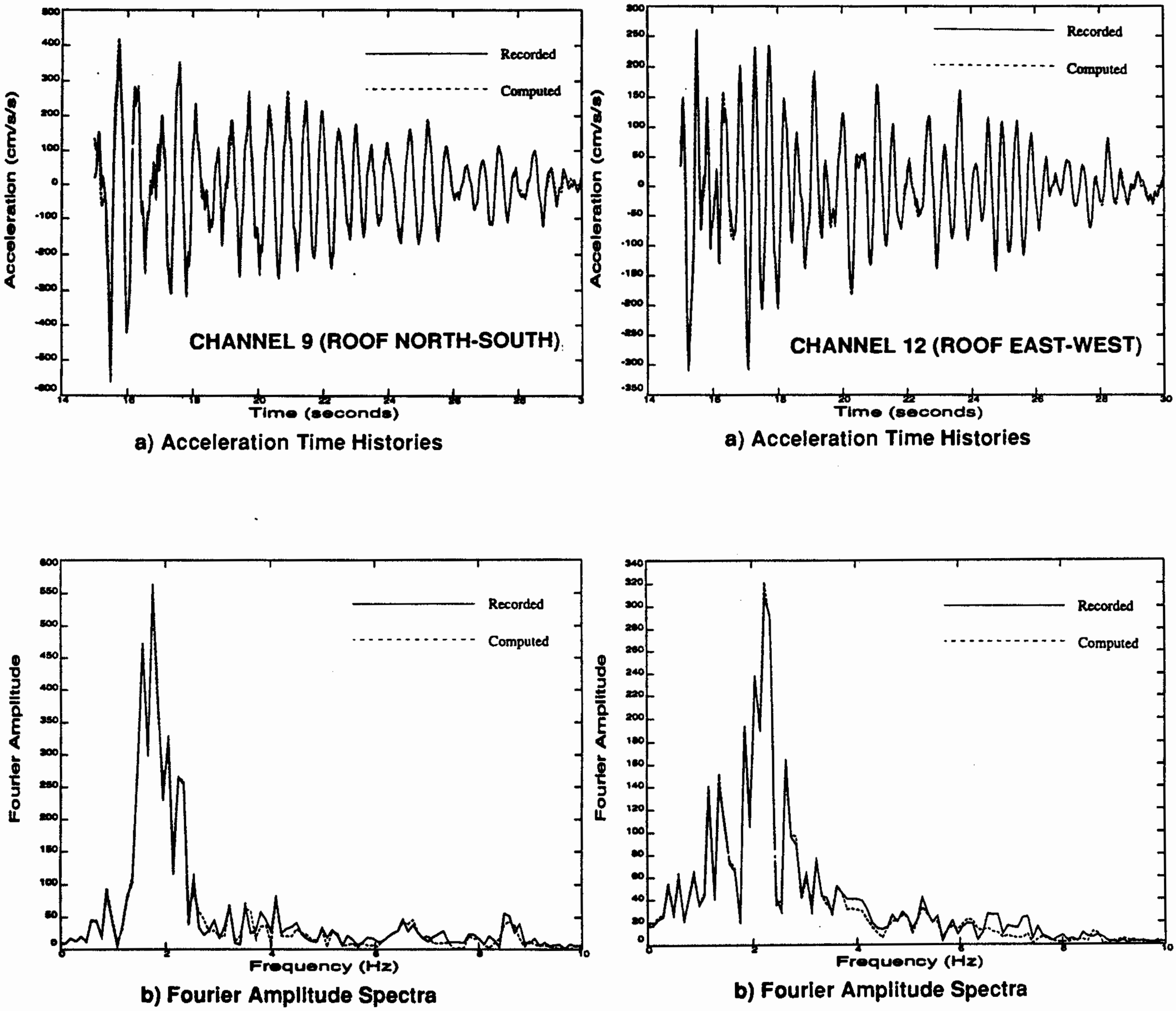

Figure 5. Comparison between Recorded Motion of Parking Structure and Computed Model Motions for the 15-30 Sec. Time Segment.

Variations in Modal Parameters between Different Time Segments

Fig. 6 shows how the period of vibration and the damping ratio for mode 1 and 2 vary over time. at different time windows. The rather small differences between these natural period and damping ratio values among all of the various time windows suggests that the parking structure did not undergo significant nonlinear response during the Northridge Earthquake.

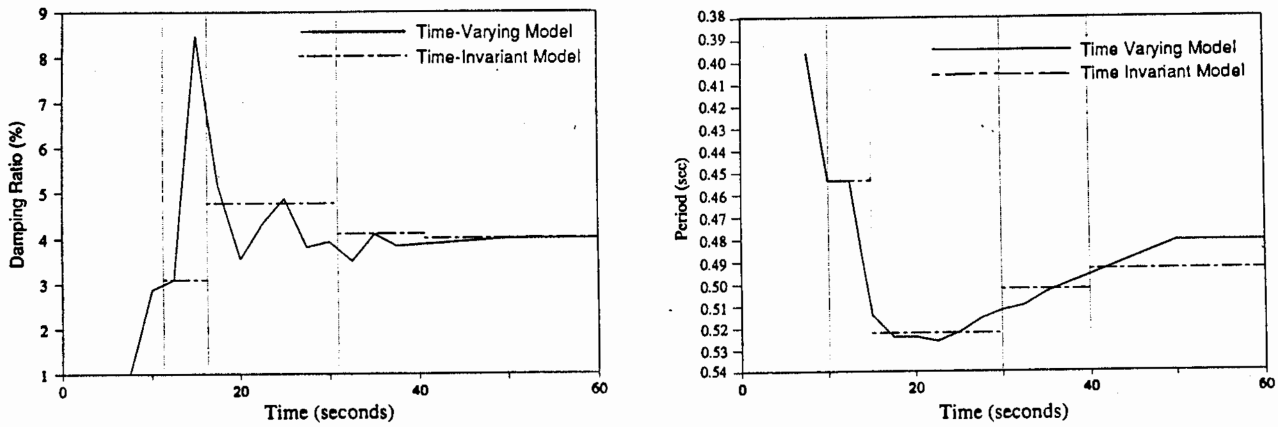

a) Mode 1: First North-South

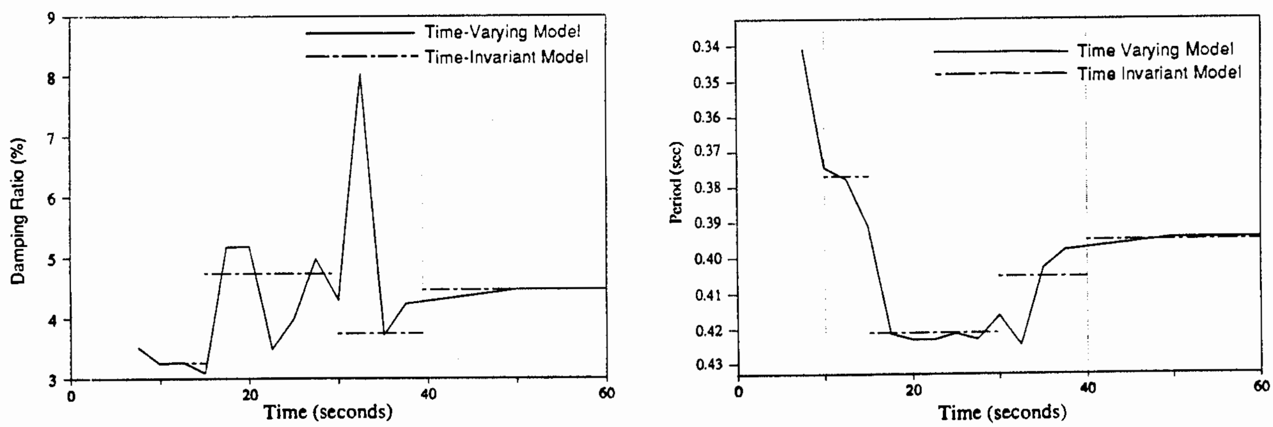

b) Mode 2: First East-West

Figure 6. Variation of Natural Periods and Damping Ratios of the Parking Structure Over Time

The variations in natural period and damping ratio between the various time windows exhibit similar trends for the two predominant modes. For both modes, the natural periods are consistently longer for the 15-30 sec. time window than for the 10-15 sec. window, and the damping ratios are consistently smaller. As the time proceeds from the 15-30 sec. window of strongest shaking to the 30-40 sec. window of decreased shaking, the natural periods for the two modes are shortened somewhat and the damping ratios are decreased. However, for both modes, the periods are still longer than those for the initial 10-15 sec. time segment, and the damping ratios are still slightly larger. A few significant peaks and irregularities are observed for the damping estimates from the time varying models which may possibly be due to the short time window duration used for these modes.

FINITE ELEMENTS COMPUTER MODELS

A detailed finite elements computer model was developed to study the dynamic behavior of the parking structure under consideration. Since the Northridge earthquake did not result in noticeable damage to the structure, only a linear model was considered using the SAP90 general finite element computer program. The model was calibrated against the structure's recorded motions, through comparison of the computed model motions and the recorded motions and comparison of the modal parameters of the finite element models against those identified by MODE-ID from the strong motion records. Once the finite element models was calibrated and checked in this way, it was used to carry out detailed analysis of the structure's dynamic response to the recorded base motions.

Fig. 7 shows the three-dimensional (3-D) plot of the finite element model that was developed for the parking structure. The general characteristics of the model are as follows: the model included 2309 nodes resulting in 13,399 equations of motion; the shear walls and ramps were modeled with shell elements, These walls were supported on soil springs with a coefficient of subgrade reaction of 300 1b/in/in, in order to incorporate soil-structure interaction. Coupling beams between the east and west walls were modeled using cracked and uncracked section properties and columns were attached to the sloped diaphragm. Hinged conditions were used at the base of the columns; the first computed 25 modes of vibration were considered producing over 99% mass participation.

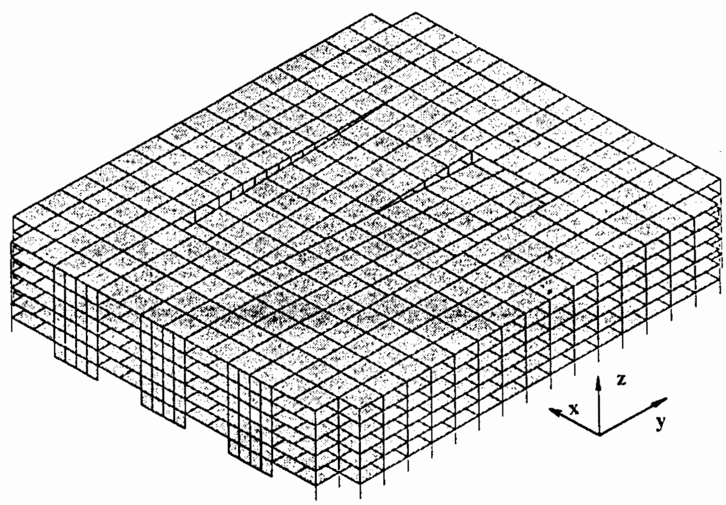

Figure 7. 3-D Finite Element Model of Parking Structure

The computer models were subjected to horizontal input motions in the north-south and east-west directions in the form of 5-percent damped response spectra. Along the north-south direction, these input motions corresponded to the average of the spectra of the recorded base motions of Channels # 3 and Channel # 4. Along the east-west direction, a response spectrum curve recorded at Channel # 5 was considered (see Fig. 3). Due to the absence of free-field vertical acceleration records, no ground shaking was considered in the vertical direction. In addition to the response spectrum analyses, transient analyses were performed using the recorded time-history motions in both directions. The standard mode superposition method and the Ritz vectors algorithm are used in SAP90 program to solve the dynamic equilibrium equations of motions for the complete structure model.

Normal Modes of Vibration

Fig. 8 shows the resulting first and third fundamental modes of the structure. Mode #1 is a lateral mode along the north-south direction (75% mass participation); the second fundamental mode is a lateral mode along the east-west direction (77% mass participation); and the third mode is a pure torsional mode. 2-D views of the significant modes along the north-south and east-west directions are shown in Fig. 9. Table 1 compares between the period of the vibrations of the first six fundamental modes obtained from Mode-ID, and computer analysis using cracked and uncracked sections. It is clear from this table that the cracked diaphragm model provides better correlation with the results obtained from Mode-ID method, particularly for the modes sensitive to in-plane diaphragm motion (i.e. Mode 1 and Mode 4).

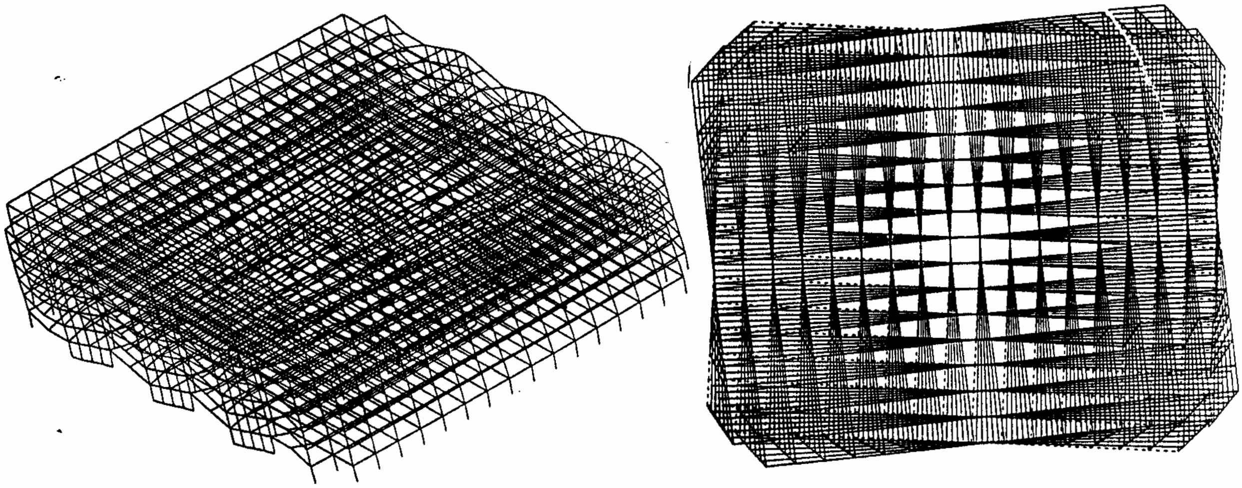

Figure 9. First Fundamental Modes acting along north-south direction, and the Torsional Mode

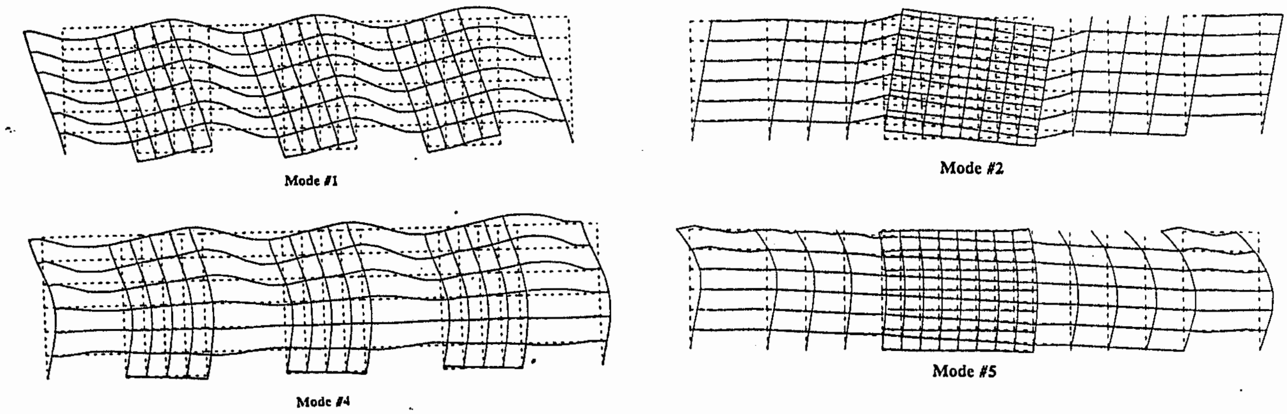

Figure 9. Two-Dimensional View of the Fundamental Modes of the Parking Structure.

Table 1
Fundamental Periods (Sec.)

Case	Fundamental Periods (Sec.)					
	Mode 1	Mode 2	Mode 3	Mode 4	Mode 5	Mode 6
Mode ID (Time Window 15-30 Secs.)	0.530	0.420	0.380	0.180	0.150	0.120
Finite Element (F. E. Model)	0.517	0.430	0.389	0.157	0.128	0.120
F. E. Model with Cracked Diaphragm	0.528	0.447	0.393	0.183	0.150	0.137

A comparison between the maximum recorded acceleration, at the locations of Channel #6 through Channel #12, is shown in Table 2. In general good results were obtained from the finite elements models.

Table 2
Comparison Between Maximum Recorded Acceleration and Computed Acceleration

Channel #	Ch. #6	Ch. #7	Ch. #8	Ch. #9	Ch. #10	Ch. #11	Ch. #12
Max. Recorded Acceleration (g)	0.32	0.34	0.22	0.58	0.84	0.55	0.31
Max. Computed Acceleration(g) (uncracked)	0.334	0.34	0.196	0.583	0.79	0.598	0.389
Max. Computed Acceleration(g) (Cracked)	0.327	0.34	0.20	0.60	0.90	0.61	0.368

The computed time history records (signatures) are plotted vs. the recorded time-history results (Fig. 10). The comparison is given for the 15-30 sec. time window of the strongest shaking. Generally, a reasonable fit between the computed and the recorded spectra curves was obtained. An excellent agreement is obtained for the building's frequencies, but there is indication of overshooting of the amplitudes at some cycles. This suggests that larger damping ratio than those obtained from the MODE-ID method would give better fit. It is also indicated that the computed response along the east-west direction is more accurate than the response obtained along the north-south direction.

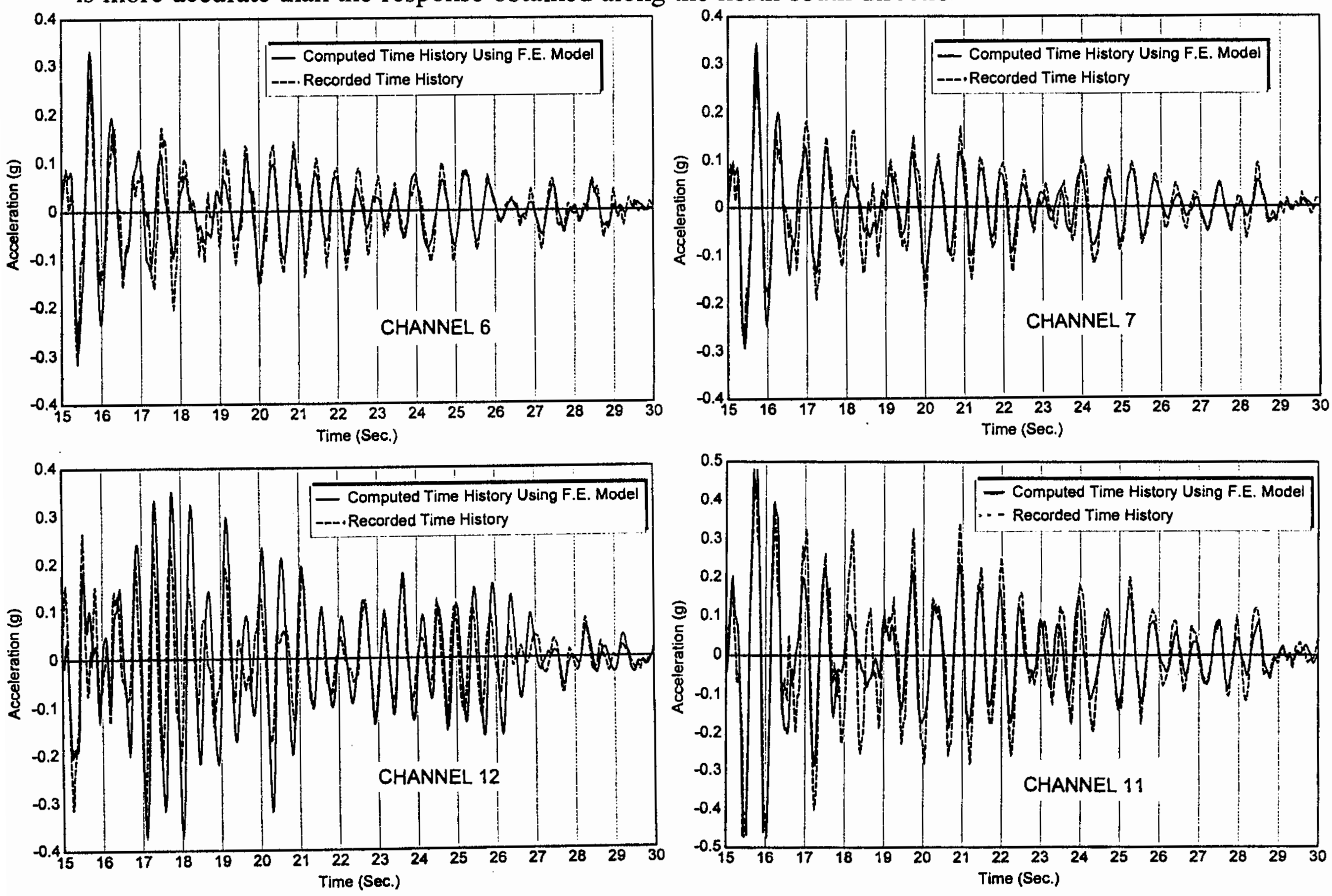

Figure 10. Comparison Between the Recorded Time History and the Computed Time History Using F.E. Model for Selected Channels.

In order to assess the structural behavior and to compare between the predicted and recorded response and the code provisions, four computer runs were performed as follows: Run #1: The finite element model was subjected to the recorded ground response curves corresponding to 5% damping. Uncracked section properties were used in this run; Run #2: This run is similar to Run #1, except that cracked sections (60% E) were used for the diaphragms and the coupling beams of the shear walls; Run #3: The model was also subjected to the UBC94 response spectrum curve for Zone 4; Run #4: The computer results were also compared with the results obtained from the UBC94 Code equivalent static lateral loads. In this regard, R_w of 8 was considered.

Table 6 shows the results of the seismic base shear obtained for the 4 cases defined above. The following observation were made: The code seismic shears are larger along the east-west direction than the north-south direction (13.2% g compared to 11.7% g). However, the finite element results using UBC code spectrum indicate different distribution (99% g along the North-South direction, and 77% along the East-West direction). It is shown that the base shear obtained from the code response spectrum curve, and the recorded ground motion are 8.46 and 5.88 times the code base shear, respectively. These factors can be compared to the reduction factor R_w = 8, which is used in UBC as a measure of the ductility of the structural system of this parking structure. As shown in Table 6 the results using the recorded ground motion as input are much smaller than the results using the UBC94 response spectrum.

Table 6
Seismic Base Shear in the Parking Structure

Case	N-S Direction E-W Direction		E-W Direction	
	V (Kips)	% G	V (Kips)	% G
F. E. Analysis Using Recorded Motions (uncracked Diaphragm)	18,567	43%	9,940	23%
F. E. Analysis Using Recorded Motions (cracked Diaphragm)	19,187	44%	10.356	24%
Finite Element Analysis UBC Spectra at Zone 4	44,084	99%	33,100	77%
Code Equivalent Static (UBC 94) with Rw = 8	5,052	11.7%	5,705	13.2%

Table 7 provides a comparison between the seismic lateral displacement at different levels of the structure. The maximum diaphragm displacements at the middle of the span of the diaphragm at the sixth level, along the north-south direction, is shown in Table 8. The following observations were made: (1) The inter-story drift based on the finite element results is approximately 0.2%, and did not result in noticeable damage to the nonstructural elements; (2) Although the ground motion did not result in noticeable damage, the maximum deflection obtained from Run #1 is approximately 2.85 times the code deflection; (3) The finite element model indicates that the north-south deflection at the mid-span of the diaphragm is approximately 16% higher than the deflection at the end shear walls.

Table 9 provides the computed seismic shear and moment demands at typical north-south and east-west reinforced concrete shear walls. This table shows that the recorded motions produced shear and flexural seismic demands that less than the capacity of the walls. This explains the absence of hair line shear cracks in these walls. In addition, there was no indication of any overstressing at the location of the construction joints at the third level (where Phase II construction started).

Table 7
Seismic Lateral Displacement in the Parking Structures

Case	F.E. with recorded motion		F.E.with cracked diaphragm		F.E.with UBC Spectrum		Code Static Rw=8	
Level	N-S wall	E-W wall	N-S wall	E-W wall	N-S wall	E-W wall	N-S wall	E-W wall
Roof	1.43"	0.74"	1.45"	0.84"	3.40"	2.63"	0.50"	0.39"
6th	1.21"	0.62"	1.23"	0.70"	2.90"	2.23"	0.43"	0.31"
5th	0.97"	0.50"	0.98"	0.56"	2.31"	1.81"	0.34"	0.24"
4th	0.71"	0.37"	0.72"	0.42	1.71"	1.36"	0.25"	0.18"
3rd	0.46"	0.24"	0.46"	0.28"	1.10"	0.90"	0.17"	0.11"
2nd	0.21"	0.12"	0.21"	0.14"	0.52"	0.45"	0.08"	0.04"

Table 8
Maximum Diaphragm Displacements (N-S)

Case	F.E. with recorded motion	F.E.with cracked model	F.E. with UBC Spectra	Code Static Rw=8
Roof	1.581"	1.663"	3.78"	0.56"

Table 9
Maximum Seismic Shear and Moment Demands on Typical N-S and E-W Walls

Wall	N-S wall				E-W wall			
Case	Seismic Shear		Seismic Moment		Seismic Shear		Seismic Moment	
	V (kips)	D/C	M (k.ft)	D/C	V (kips)	D/C	M (k.ft)	D/C
F. E. Analysis Using recorded Motion	2244	0.96 *	59,160	0.69	5110	0.73	208,334	0.56
F. E. Analysis Using UBC Spectra	5328	2.28 *	142,604	1.65	16586	2.36	676,211	1.80
Code Equivalent Static Rw = 8	842	0.84 **	36,585	0.595	2852	0.95	123,940	0.33

* indicates using $\phi = 1$, ** indicates using $\phi = 0.6$ and factored load.

Table 10 indicates that the shear walls experienced noticeable uplift. Maximum uplift forces of 2225 kips and 1763 kips in the east-west walls and north-south walls, exceeded the estimated 1210 kips uplift resistance forces. It is noted that the code uplift forces are less than the uplift resistance forces, indicating that code stress checks will not predict this uplift behavior.

Table 10
Maximum Seismic Uplift Forces and Displacements

Wall	**N-S middle wall**		**E-W wall**	
Case	**Uplift force**	**Uplift disp.**	**Uplift force**	**Uplift disp.**
Finite Element Analysis Using recorded Motion	1763 kips	0.29"	2225 kips	0.31"
Finite Element Analysis Using UBC Spectra	4230 kips	0.68"	7444 kips	1.05"
Code Equivalent Static Rw = 8	627 kips	0.10"	1143 kips	0.16"

Note: Uplift forces in this table do not include reduction due to gravity loads

A stress check was performed to assess the seismic behavior of the short columns created due to the sloped ramps configuration. The result of this investigation for some critical short columns, indicated that the column's seismic shear demand forces due to the recorded input motions did not exceed their ultimate strength capacity, i.e., the demand/capacity ratio less than 1.0. However, higher levels of seismic shaking, due to the UBC response spectrum, will result in overstressing of these columns with demand/capacity ratio of approximately 2.5. This may be critical and could result in shear failure of these nonductile columns (Ref. 6). Typical column details, show limited tie reinforcements of #3 @ 12" o.c. New code provisions for gravity columns require minimum ties of #4 @ 6" o.c.

Another stress check was performed to examine the upper coupling beams connecting the N-S shear walls. It is shown that these beams were overstressed using the response spectrum analysis using the recorded response spectrum curves, with shear D/C of 2.84 and the flexural D/C of 1.94. The proposed ATC-33 (Ref. 7) recommends the use of limiting D/C ratios for shear and flexure as 1.0 and 2.0, respectively, for immediate occupancy performance. Therefore, higher D/C ratios may be justifiable in this case, based on the adequate performance of these long coupling beams during the Northridge earthquake .

One important assessment for this particular parking structure, is to study the integrity of the connections between the precast concrete columns and the floor slab. Table 11 provides the results of the stress check of some of the critical connections. D/C ratios up to 2.18 were obtained using the finite element model with recorded ground motion. However, no indication of overstressing was found during the site review. It is also indicated in Table 11 that D/C ratios up to 5.25 can be obtained at some of these connections, when using the Code response spectrum. It is highly questionable that these connections will sustain such large demands without experiencing excessive damage. Failure of these connections may lead to the separation of the columns from the slab, which may result in columns' instability (Ref. 8)

Table 11
Maximum Pull Forces At Selected Column-Slab Connections

Forces	Conn. # 1		Conn. # 2		Conn. # 3		Conn. # 4	
Case	P (kips)	D/C	P (kips)	D/C	P (kips)	D/C	P (kips)	D/C
F. E. using Recorded Motion.	116	2.18	91	1.72	76	1.43	73	1.37
F. E. Analysis Using UBC Spectra	278	5.25	219	4.13	227	4.28	217	4.09
Code Equivalent Static Rw = 8	35	1.03	31	0.91	40	1.18	38	1.12

Connection # 1: For Column at Grid (7) and (C) @ 2nd Level South Ramp.
Connection # 2: For Column at Grid (8) and (C) @ 2nd Level South Ramp.
Connection # 3: For Column at Grid (6) and (B) @ 5th Level., Connection # 4: For Column at Grid (6) and (B) @ 4th Level .

RESPONSE OF VERTICAL VIBRATION OF THE ROOF GIRDER

In order to measure the vertical acceleration at the top level of the parking structure, one of the sensors was installed at the middle of the 65-foot long upper girder at the roof (Channel #13). A two-dimensional computer model was prepared to model the vertical response of the girders. Fig. 11 shows the first fundamental mode shape (estimated as 0.29 seconds). The following observations were made: (1) For large span girders (65 ft long), effective floor vertical acceleration in the middle of the girder can be significant (up to 3.5 times the peak ground vertical acceleration). This can lead to shear overstressing at the end of the beams (Ref. 7); (2) The acceleration of the nonstructural elements that may be attached at the middle of the long span girder (e.g. piping, etc) with fundamental periods between 0.20 to 0.40 seconds, can be significant; and (3) The current building codes do not provide simplified formulas to consider the effect of the vertical acceleration on the floor girders or beams. It appears that guidelines to consider such an effect are required. One design approach would be to increase or decrease the gravity loads acting on the beam with 2.5 times the peak ground vertical acceleration (in %g) times the gravity loads.

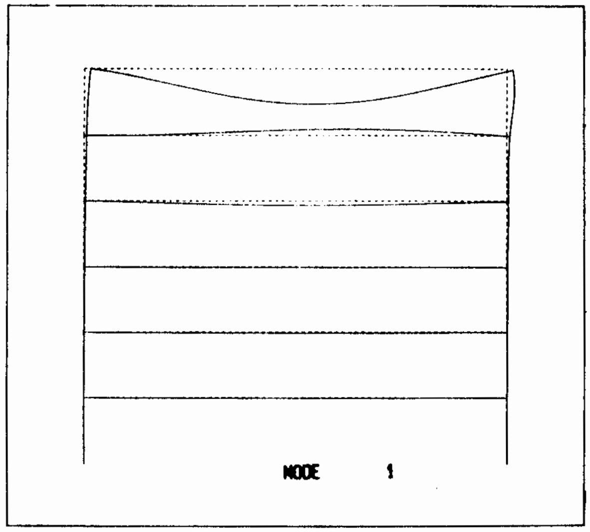

Figure 11. 1st Fundamental Mode Shape of Roof Girder

RESPONSE OF THE ROOF PARAPET

In order to measure the out-of-plane acceleration at the roof parapet of the parking structure an accelerometer (channel # 14) had been installed at the top of the north roof parapet, and recorded very strong shaking (with a peak acceleration of 1.21 g). A three-dimensional computer model was developed to model the interaction between the parapet and the parking structure. Ten line elements were used to model the parapet. Other line elements were used to model the vertical beam and edge beams. Lumped masses were used at the nodes of the parapet elements. Uncracked sections were used for section properties. A transient analysis using Channel # 10 record as an input motion; 5% damping was considered. The result of the finite element analysis indicated that the first and second mode shapes provide for over 99% of the mass participation (78.6% and 21.3%, respectively). The first fundamental period is 0.079 seconds, and the second mode is 0.016 seconds.

Fig. 12 shows Mode # 1 and a comparison between the recorded and generated linear time history for the out-of-plane top acceleration. It is shown that an excellent prediction of the behavior can be obtained using the analytical model. A comparison between the stresses required by UBC94 Code provisions, and the recorded stresses scaled to an Upper Level event indicated that in this building the design of the parapet, based on the code formula, is conservative and should produce satisfactory results.

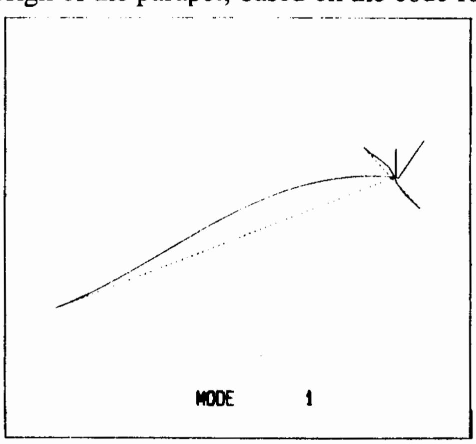

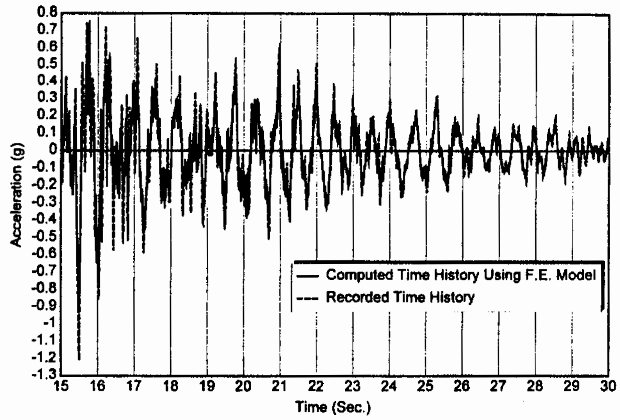

Figure 12. Mode Shape and Comparison Between Recorded and Generated Time History for Roof Parapet

CONCLUSIONS

The following are the main conclusion of the study presented in this paper:

(1) The system identification resulted in models whose computed motions compared very closely to the parking structure's recorded earthquake motions. The model parameters that were estimated showed that: (a) the structure's response was dominated by its first north-south and first east-west translational modes of vibration in its two principal directions, together with its pseudostatic response component; (b) rocking of the structure about its base was an important contributor to its east-west translational response (and possibly to its north-south response as well, although rocking in the north-south direction was not explicitly measured by the current array of strong motion instruments at the structure); (c) the variations in the structure's estimated modal properties over the duration of the shaking suggests that nonlinear behavior was not a strong contributor to this parking structure's seismic response during the Northridge earthquake; and (d) Damping ratios varying from 4% to 5% of critical were estimated for the structure's significant modes of vibrations during the time window of strongest ground shaking.

(2) The finite element computer model described in this report was able to reasonably predict the main dynamic characteristics of the structure. It is clear that the cracked diaphragm model provides better correlation with the results obtained from MODE-ID method, particularly for the modes sensitive to in-plane diaphragm motion (i.e. Mode 1 and Mode 4 which correspond to the modes in the north-south direction).

(3) The finite elements results indicated that possibly, at a higher level of ground shaking, the drift ratio may exceed the value recommended by the current provisions of the code which is based on the $3(R_w/8)$ factor. Therefore, an increase of this factor to reflect the nonlinear response of the structure at higher levels of ground shaking is recommended. The results also indicated that the maximum uplift forces at the end of the shear walls during the Northridge earthquake exceeded the estimated uplift resistance forces. It is noted that the code stress checks will not predict this uplift behavior.

(4) The finite element results indicate that the roof probably experienced flexural cracking, and provided more flexible response, with a slight increase in the seismic forces. The finite element model indicates that diaphragm deflection is approximately 10% higher than the deflection at the end shear walls. Finite element mode with cracked diaphragms, indicate that this ratio increases to 16%.

(5) The study of the coil inserts connecting the precast columns and the concrete floors indicated that D/C ratios up to 5.25 can be obtained at some of these connections, when using the Code response spectrum. It is highly questionable that these connections will sustain such large demands without experiencing excessive damage. Failure of these connections may lead to the separation of the columns from the slab, which may result in columns' instability.

(6) For large span girders (65 ft long), effective floor vertical acceleration in the middle of the girder can be significant (up to 3.5 times the peak ground vertical acceleration). This large acceleration produces significant vertical loading that should be included in the design. Both the increase and the decrease of the total loads action on the girder should be considered. One design approach would be to increase or decrease the gravity loads acting on the beam with 2.5 times the peak ground vertical acceleration (in %g) times the gravity loads.

(7) A computer model was able to predicted the large acceleration recorded at the top of the roof parapet at the north side of the parking structure. It was shown that in this building the design of the parapet, based on the code formula, is conservative and should produce satisfactory results.

ACKNOWLEDGMENT

Professor James Beck of California Institute of Technology was consultant to the project, and provided invaluable assistance. This research was sponsored by the Strong Motion Instrumentation Program (SMIP), of the California Department of Mines and Geology. Dr. Moh Huang of SMIP provided useful suggestions during the project. Any opinions, findings, and conclusions or recommendations expressed in this paper are those of the writers and do not necessarily reflect of the views of the sponsors.

REFERENCES

(1) Holmes, W. T. and Somers, P. " Northridge Earthquake of January 17, 1994 Reconnaissance Report, Vol. 2", Earthquake Spectra, Supplement C to Volume 11, January 1966, pp. 75-98.

(2) Beck, J.L." Determining Models of Structures from Earthquake Records", Report No. EERL 78-01, Earthquake Engineering Research Laboratory, California Institute of Technology, Pasadena CA., June 1978.

(3) Beck, J.L. "Statistical System Identification of Structures", Structural Safety and Reliability, ASCE, New York, Aug 1990, pp 1395-1402.

(4) Werner, S.D., Beck, J.L., and Levine, M.B. "Seismic Response Evaluation of Meloland Road Overcrossing using 1979 Imperial Valley Earthquake Records", J. of Earthq. Eng. and Struct. Dyn., Vol. 15, No. 2, Feb.1987, pp. 249-274.

(5) Werner, S.D., Beck, J.L., and Nisar, A. "Dynamic Tests and Seismic Excitation of a Bridge Structure" Proc. of Fourth U.S. Nat. Conf. on Earthq. Eng., Palm Springs, CA., Vol. 1, May 20-24, 1999, pp. 1037-1046.

(6) Porush, A., Hilmy, S. and Grigorian, C. "CSUN Parking Structure C, Causes of Failure and Code Issues", Proceedings of the 1995 SEAOC Convention, Idian Wells, California, October 19-21, 1995.

(7) Guidelines for the Seismic Rehabilitation of Buildings, ATC-33.03, The Applied Technology Council, 75% Complete Draft, October 1995.

(8) Hilmy, S . and Porush, A."Seismic Strengthening of Non-ductile R/C Gravity Columns, Retrofit Strategies and Code Considerations", Proceedings of the Second Cairo Earthquake Engineering Symposium on Seismic Design Codes, December 1995, Cairo, Egypt.